

THE 4TH INTERNATIONAL CONFERENCE ON ALUMINUM ALLOYS

THREE POINT BENDING OF AA7108 - INFLUENCE OF MICROSTRUCTURE AND SPECIMEN GEOMETRY

H.J. Roven¹ and T. Iveland²

1. The Norwegian Institute of Technology, Department of Metallurgy, 7034 Trondheim, Norway
2. SINTEF, Materials Technology, 7034 Trondheim, Norway

Abstract

The aim of the present work was to establish empirical knowledge for the alloy AA 7108 in view of bending processes in general and in the scope of an ongoing implementation of this experience during development of physically sound material models to be used in computer simulations. Laboratory three point bending tests were considered helpful in order to study the basics in this regard. Specimen orientation and deformation rate were variables and local strains were measured after deformation applying a fine 500 μm surface grid. In addition, tensile tests varying the specimen orientation (texture effect), strain rate and specimen width over thickness (w/t- ratio) were employed in order to reveal a "ranking of importance" of these variations on the plastic flow and hence formability and elastic relaxation (spring-back).

Introduction

The application of aluminium extrusions in the automotive industry depends on the development of new alloys, product design and process optimization, e.g. /1/. Among the traditional parts made from aluminium extrusions is the light weight, energy absorbing bumpers (7xxx-series). Today aluminium companies and the automobile industry are upgrading the use of bent profiles for extensive applications (space-frame structures). As a part of one R&D programme focusing on bending of 7xxx-alloys, the present work is emphasizing the microstructural and geometrical aspects. The effects of deformation rate, e.g. /2-4/, and crystallographic texture /5-7/ on plastic deformation are well described in the literature. Further, strain gradients which are characteristic of bending, are known to influence the work hardening and hence the stress vs. strain relationship /8/. However, details relating microstructure, texture, geometry and deformation by bending are not fairly understood. Therefore, in the present work the effects of deformation rate and test orientation are studied by means of laboratory three point bending tests including grid pattern strain analyses combined with tensile tests varying the specimen geometry, orientation and loading rate.

Experimental procedure

The high strength aluminium alloy AA 7108 with the chemical composition (by wt%): 5.2 Zn, 1.2 Mg, 0.2 Zr, 0.15 Fe, 0.1 Si and balance Al was used in the present study. The extruded plate having a thickness $t = 8.0$ mm was supplied by Raufoss AS in the as extruded condition. Due to the thermally stable Zr-containing dispersoids, the grain structure was generally non-recrystallized, although a ~ 30 μm surface zone contained recrystallized grains. The material was characterized by a marked crystallographic rolling-type texture comprising the S, Brass, Cu and Cube components and the primary particles were aligned into the extrusion direction.

Three point bending specimens were prepared in full thickness of the plate. The specimen width over thickness ratio was constant ($w/t = 2$) and the geometrical dimensions $t = 7.8$ mm, $w = 16.0$ mm and $l = 50$ mm. Two different specimen orientations were machined with their length (i) parallel to the transverse (T) or (ii) parallel to the longitudinal (L) direction of the plate. Before testing each specimen was given a solution heat treatment, $480^\circ\text{C}/30$ min., before quenching in water. In order to avoid natural ageing, all tests were carried out within ~ 10 minutes after solution heat-treatment. Standard three point bending was carried out at constant displacement rates 6.25 mm/s and 6.25×10^{-2} mm/s using a general purpose bend fixture mounted in a servohydraulic MTS machine. The distance between the supports was 41.5 mm and the diameter of both the support rolls and the stamp roll was 6.5 mm. No lubrication was used in order to reduce frictional forces. All tests were stopped at ~ 11 mm total displacement followed by controlled unloading.

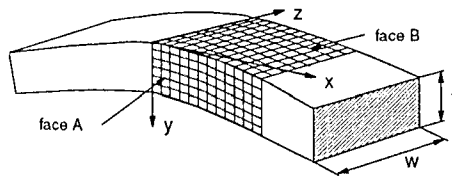


Figure 1. Sketch of specimen with grid pattern and the corresponding axes system used. Sideface (A) and top tensile face (B).

Specimens both with the L and the T orientation were deformed with a mechanically polished surface finish and with squared grids introduced on two orthogonal faces (face A and face B), see Figure 1. The spacing between the grid lines was ~ 0.5 mm and the line thickness was ~ 10 μm . From the displaced grid pattern it was possible to calculate nominal plastic strains after testing along the original axes system.

Due to different microstructures, and thereby texture variations, in the near surface and in the bulk of the extrusion, rectangular tensile specimens having a 4 mm thickness were machined from the center part of the 8 mm thick material. All specimens had a 30 mm gauge length and the width over thickness ratios (w/t) 1, 3 and 5 were used in order to study the influence of the specimen geometry on the stress versus strain relationships. The anisotropic plastic flow was characterized employing specimens taken 0° , 55° and 90° to the extrusion direction. The 55° orientation was motivated from the fact that isotropic materials usually form localized necking and have a zero normal strain in this direction with respect to the tensile axis /9/. All specimens were solution heat treated at $480^\circ\text{C}/30$ min. and tested within 15 minutes after

quenching in water. Two ramp rates (6.25 mm/s and $6.25 \times 10^{-2} \text{ mm/s}$) giving initially strain rates $\dot{\epsilon} \approx 1.8 \times 10^{-3} \text{ s}^{-1}$ and $\dot{\epsilon} \approx 0.18 \text{ s}^{-1}$, were used in order to establish flow curves that correspond directly to the previously described bending tests.

Experimental results

Plastic deformation by three point bending comprehends both tensile and compression flow. In order to understand the deformation process it is necessary also to study the details of the tensile flow behavior. In the following, the results from the tensile tests are therefore presented before the observations made during the bending experiments.

Anisotropic tensile properties. The crystallographic texture is responsible for pronounced anisotropic tensile properties. As an example, uniaxial tensile curves from three different specimen orientations at constant w/t -ratio and an initial strain rate of $\dot{\epsilon}_{\text{init}} \approx 0.18 \text{ s}^{-1}$ are presented in Figure 2. The work hardening rate and σ_{UTS} is significantly larger in the 0° and 90° than in the 55° orientation. Hence, the latter orientation is softer and has a larger uniform strain ϵ_u than, in increasing order, the 90° and 0° orientations. The formability is often closely related to the the uniform strain ϵ_u , i.e. the strain at the onset of plastic instability in tension where $d\sigma/d\epsilon = \sigma$. This parameter may be incorporated into a quantity $\Omega = [(\sigma_{\text{UTS}} - \sigma_0)/\epsilon_u]$ which will vary with the specimen test orientation if the material contains a chrystallographic texture. In Figure 2(b) a normalized quantity, $(\Omega)/(\Omega)_{0^\circ}$, is invented to demonstrate strong anisotropic behaviour focusing on the work hardening potential in the uniform strain regime and on the uniform strain value itself under constant specimen geometry and ramp rate conditions. Obviously, the texture influence is more significant at 55° than at 90° .

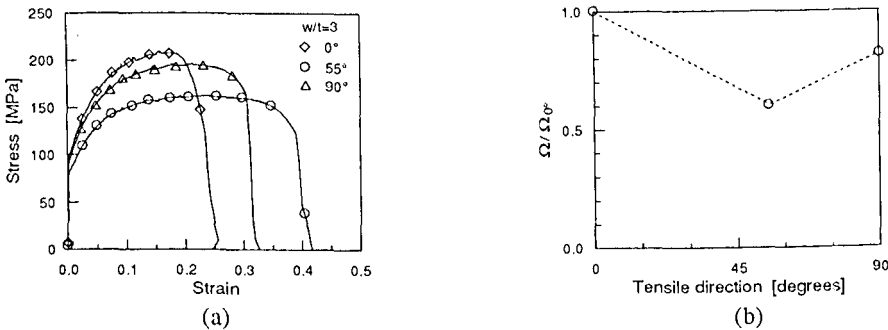
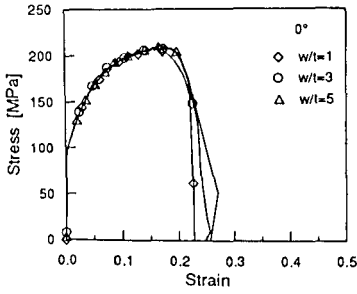
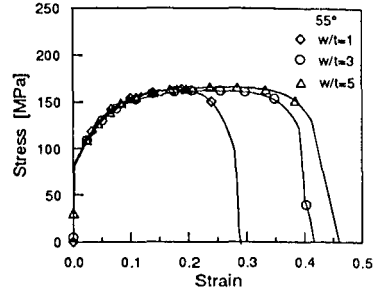


Figure 2. (a) Uniaxial engineering tensile curves for specimens oriented 0° , 55° and 90° to the extrusion direction. (b) Dimensionless Ω/Ω_{0° against specimen test orientation ($\Omega = [(\sigma_{\text{UTS}} - \sigma_0)/\epsilon_u]$). [$w/t = 3$ and $\dot{\epsilon}_{\text{init}} \approx 0.18 \text{ s}^{-1}$]

Influence of tensile specimen geometry. The geometrical influence on tensile flow is, although influenced by the specimen orientation, quite pronounced as can be seen from Figure 3(b). Specimens oriented parallel to the extrusion direction do not show such a geometrical effect within the uniform strain regime, but the value of ϵ_u may increase somewhat with increasing w/t -ratio.



(a)

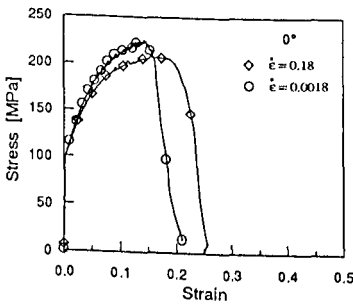


(b)

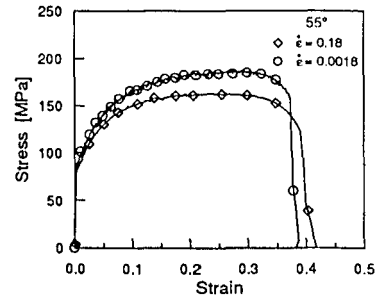
Figure 3. Uniaxial engineering tensile curves from specimens with w/t ratios 1, 3 and 5. Tensile direction (a) 0° and (b) 55° to the extrusion direction. [$\dot{\epsilon}_{init} \approx 0.18 \text{ s}^{-1}$]

The main effect of increasing the w/t ratio within the two other specimen test orientations, i.e. 55° and 90° , is to enhance the uniform (ϵ_u) and the fracture strain (ϵ_f). This observation is valid for both ramp rates used. Another important effect due to the specimen geometry is related to the anisotropic behavior. A larger w/t ratio will increase the anisotropy as illustrated by Figure 5(a).

Strain rate effects in tensile tests. All tensile test results presented above refer to an initial strain rate $\dot{\epsilon}_{init} \approx 0.18 \text{ s}^{-1}$. By lowering the initial strain rate by a factor of hundred to $\dot{\epsilon}_{init} \approx 1.8 \times 10^{-3} \text{ s}^{-1}$, the following observations are of importance. The effects of the initial strain rate $\dot{\epsilon}_{init}$ in the 0° versus the 55° and 90° orientations differ from each other (for comparison of the extremes 0° and 55° , see Figure 4). At 0° test orientation a high strain rate lowers the σ_{UTS} and increases ϵ_u . In opposite, at 55° and 90° orientations, the highest strain rate lowers the σ_{UTS} and decreases ϵ_u . Generally, increasing the strain rate reduces the anisotropic behaviour. These findings are valid for all three w/t-ratios used.



(a)



(b)

Figure 4. Uniaxial engineering tensile curves illustrating the strain rate effect at constant w/t=3 for (a) 0° and (b) 55° test orientations.

In order to compare simultaneously the effects of strain rate, specimen orientation and the geometrical w/t-ratio, the dimensionless parameter $\psi = [\Omega_{\dot{\epsilon}_1} / \Omega_{\dot{\epsilon}_2}]$ is plotted for the three test orientations, Figure 5(b). (Here: $\Omega_{\dot{\epsilon}_1}$ and $\Omega_{\dot{\epsilon}_2}$ refer to the lowest and the highest strain rate,

respectively). As can be seen, the effect of strain rate on Ω (which physically represents the linear slope from σ_0 to σ_{UTS}), is quite pronounced at 0° but is also existing at 55° and 90° . At 55° the strain rate and the w/t -ratio effect on Ω is of the same order. At test orientations 0° and 90° the w/t -ratio is having less influence on Ω as compared to the strain rate.

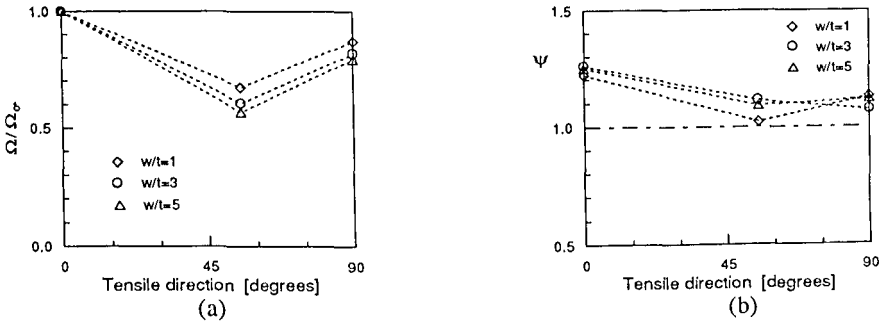


Figure 5. (a) Dimensionless Ω/Ω_0 against specimen test orientation for $w/t = 1, 3$ and 5 ($\Omega = [(\sigma_{UTS} - \sigma_0)/\epsilon_u]$, $[\dot{\epsilon}_{init} \approx 0.18 \text{ s}^{-1}]$). (b) Dimensionless parameter $\Psi = [\Omega_{\dot{\epsilon}_1} / \Omega_{\dot{\epsilon}_2}]$ as function of the test orientation for w/t -ratios 1, 3 and 5.

A traditional way of presenting strain rate effects, is through the strain rate sensitivity parameter (m), defined by the equation

$$\sigma = C (\dot{\epsilon})^m \quad (1)$$

at constant T and ϵ (C is an experimental constant).

The three plots in Figure 6 indicate that m is having a more negative value with increasing ϵ and also by increasing the w/t -ratio beyond 1. Further, the m -value is almost independent of the specimen test orientation.

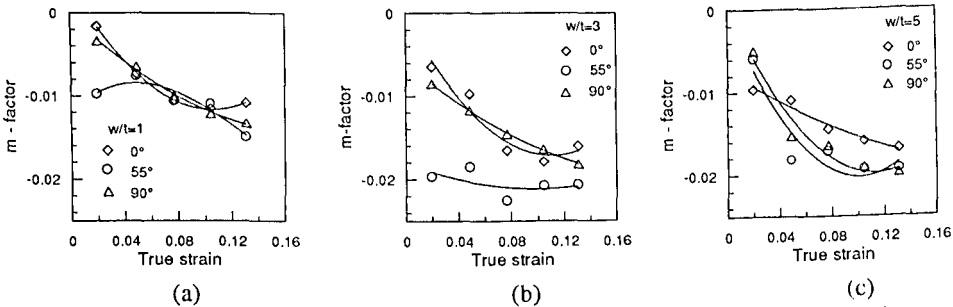


Figure 6. Strain rate sensitivity m as a function of ϵ for $0^\circ, 55^\circ$ and 90° test orientations. (a) $w/t = 1$, (b) $w/t = 3$ and (c) $w/t = 5$.

Influence of specimen orientation and deformation rate in bending. By varying the specimen orientation in bending one may expect to reveal some effects of the crystallographic texture. In the present case, the anisotropic effect on the load versus displacement curves is relatively

small. In contrast to the tensile curves (Figure 2(a)), specimens oriented 90° to the extrusion direction are slightly displaced towards higher load levels as compared to the longitudinal direction. A more significant influence on the curves is attributed to the rate of deformation, i.e. the curves obtained at higher rates fall below those of the lower deformation rate (Fig. 7).

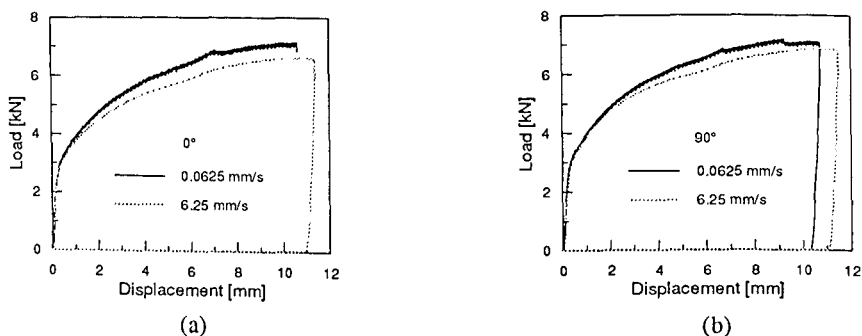


Figure 7. Three point bending load versus displacement curves showing the effect of deformation rate (ramp rates 6.25×10^{-2} mm/s and 6.25 mm/s). Specimens having the orientation (a) L and (b) T. [$w/t=2.0$]

However, a very significant *consequence of the anisotropic flow* revealed by comparing the two test orientations is related to the unloaded *geometrical shape* of the specimens. The transverse specimens have demonstratively larger shape change in the transverse (z-direction) of the cross section plane located in the specimen half-length, than in the specimen having the L orientation. On the tensile face the total $e_z = -5.9\%$ for L and $e_z = -10.7\%$ for the T orientation, thereby representing a difference by a factor of ~ 2 . Similarly, on the compressive side is the total $e_z = 4.4\%$ for L and $e_z = 8.2\%$ for specimens of T-orientation (once again a factor of ~ 2). This finding is independent of the deformation rate and is illustrated by the sketch in Figure 8.

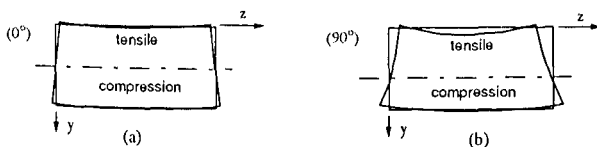


Figure 8. Sketch of the cross section geometry in the specimen half-length after bending to a displacement of ~ 11 mm showing the significant effect of specimen orientation. (a) L orientation and (b) T orientation.

These observations of macroscopic character are supported by the more detailed strain analysis obtained from the grid patterns: (i) At the high deformation rate the specimen orientation has a marked effect on the actual local strains acting both on face A and on face B. In the position corresponding to the specimen half-length (i.e. $x=0$), and on the face A, the maximum tensile strain (e_x^*) for the T orientation is a factor 1.2 larger than the corresponding maximum tensile strain for orientation L (Figure 9). (ii) On the tensile face B, both e_x and e_z strains revealed differences between the two specimen orientations. The L orientation has roughly constant strain values (both e_x and e_z) along the z direction, i.e. e_z/e_x varies between 0.4-0.6

only (both deformation rates). In opposite, specimens of the T orientation have at both deformation rates larger strain values at the specimen edges (both e_x and e_z) and roughly a factor 0.5 lower strains (both e_x and e_z) in the half-width part on face B (Figure 10). This implies that the e_z/e_x ratio along the z direction varies between 0.3 and 0.8, i.e. a geometrical curvature exists in the z-direction (Figure 8). In spite of these differences, the extension of the plastic zone in the x direction on face A is independent of the specimen orientation. Further, the neutral axis is displaced $\sim 0.83\text{mm}$ and $\sim 0.78\text{mm}$ towards the compression side for the L and T orientation, respectively, i.e. the same amount and also independent of the specimen orientation.

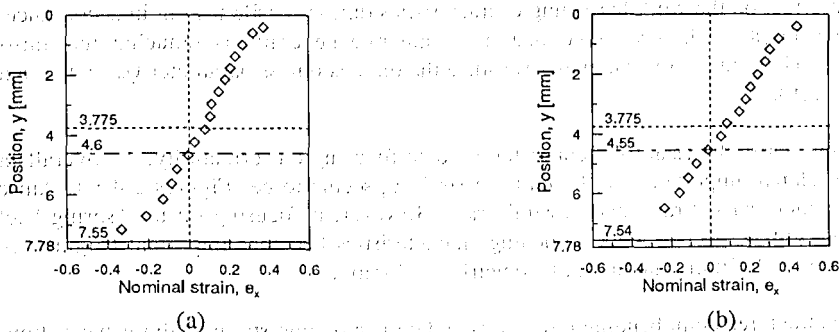


Figure 9. Measured nominal strains, e_x , at different positions y on face A in the specimen half-length position ($x=0$). Specimen of orientation (a) L and (b) T. Also shown are the values of the physical half thickness after bending (3.775mm) and the positions of the displaced neutral axes. [Ramp rate 6.25 mm/s]

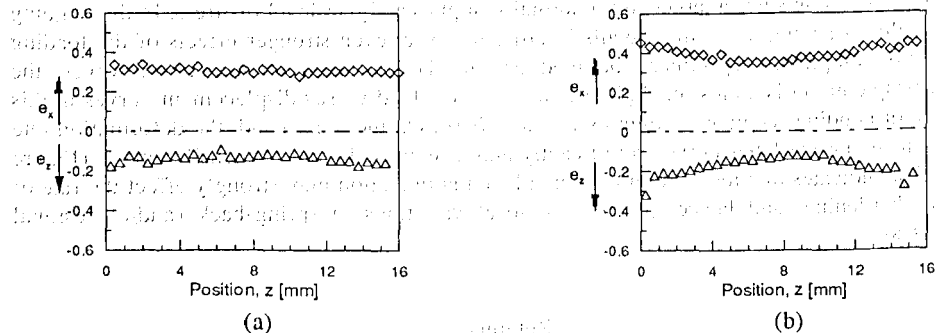


Figure 10. Measured strains on the tensile face B after bending. Note difference between the specimen of orientation (a) L and (b) T. [Ramp rate 6.25 mm/s]

Discussion and Conclusions

The aim of the present work was to establish empirical knowledge for the alloy AA 7108 in view of bending processes in general and later to implement this experience during the development of physically sound material models to be used in computer simulations. Laboratory three point bending tests were considered useful for studying the basics in this regard. Besides being in general agreement to the established knowledge associated with plastic deformation, i.e. [2-7], the present observations demonstrate that tensile test results to

be used as input in computer simulations of bending nonrecrystallized 7xxx alloys must be selected carefully. First of all, the anisotropy (in terms of the parameter Ω) of $\sigma - \epsilon$ curves is very pronounced and this anisotropy is magnified by increasing the w/t ratio of the test specimen (Figure 5(a)). Secondly, the strain rate sensitivity increases with strain and specimen w/t-ratio but is roughly isotropic (Figure 6). However, the effect of the tensile test strain rate is more important than the w/t-ratio effect at tensile directions 0° and 90° to the extrusion direction (Figure 5(b)). But, in the softer 55° direction the magnitude of influence from the strain rate and from the w/t-ratio is of the same order (Figure 5(b)). However, the w/t-ratio has no effect on the work hardening characteristics during tensile testing in accordance to the findings in /8/. It is also noted that the strain rate generally is reducing the anisotropic behavior (in terms of the parameter Ω) since the dimensionless parameter $\psi_{0^\circ} > \psi_{55^\circ}$ and ψ_{90° , Figure 5(b).

With respect to the establishment of tensile data focusing on formability, the overall ranking of the relative importance to the uniform strain ϵ_u seems to be (Figures 2-4): 1. Anisotropy and geometrical w/t-ratio and 2. Strain rate. However, if focusing on the "spring-back" the ranking with respect to work hardening characteristics becomes important (Figures 2-4): 1. Anisotropy, 2. Strain rate and 3. Geometrical w/t-ratio.

Finally, the three point bending test results and corresponding strain analyses have shown that *the angle of loading with respect to the extrusion direction* (anisotropy) has a very important impact on the geometrical shape of the plastically formed specimen (Figure 8) and hereby also on the local strains operating on the bent body (Figure 10). The latter underlines the possibility of having severe orientational differences in the local spring-back (and/or residual stresses) during unloading since a larger strain normally implies a higher level of stress. In the ongoing work this is studied in further details in order to reveal even stronger effects of the loading direction employing specimens oriented 55° to the extrusion direction. However, the anisotropic effect is almost negligible in terms of the load versus displacement curves in this mode of bending (comparing Figures 7(a) and 7(b)). On the other hand, the deformation rate is influencing the latter curves significantly and as expected from the tensile curves (Figure 4). This indicates that local strain rates in a bending operation may strongly effect the rate of work hardening, and hence give rise to local variations in spring-back (and/or residual stresses).

References

- /1/ M.Isogai and S. Murakami, Journ. of Materials Processing Techn., 38, (1993), 635-654
- /2/ W.G. Johnston and D.F. Stein, Acta Metall. 11, (1963), 317-318
- /3/ D.H. Avery and W.A. Backofen, Trans. Am.Soc.Met. 58, (1965), 551-562
- /4/ E.W. Hart, Acta Metall. 15, (1967), 351-355
- /5/ G.I. Taylor, I.Inst. Metals, 62, (1938), 307-324
- /6/ G. Sevillano, Pan Houtte and E. Aernoudt, Progress in Materials Science, 25, (1981), 69-412
- /7/ G.Y. Chin and W.L. Mammel, Trans. Metallurgical Soc. AIME, 239, (1967), 1400-1405
- /8/ N.A. Fleck, G.M. Muller, M.F. Ashby and J.W. Hutchinson, Acta Metall. 42, (1994), 475-487
- /9/ S.F. Keeler and W.A. Backofen, Trans.Am.Soc.Met., 56, (1963), 25-48